ChemPubSoc Europe

DOI: 10.1002/chem.201501533

CHEMISTRY A European Journal Communication

Carbocatalysis

Graphenes as Efficient Metal-Free Fenton Catalysts

Juan C. Espinosa,[b] Sergio Navalón,[b] Ana Primo,[b] Mónica Moral,[c] Javier Fernández Sanz,[c] Mercedes Álvaro,[b] and Hermenegildo García*[a]

Abstract: Reduced graphene oxide exhibits high activity as Fenton catalyst with HO• radical generation efficiency over 82% and turnover numbers of 4540 and 15023 for phenol degradation and H_2O_2 consumption, respectively. These values compare favorably with those achieved with transition metals, showing the potential of carbocatalysts for the Fenton reaction.

The vast majority of chemical processes at industrial scale are catalytic and most of them use transition metals as active sites.[1] For the sake of sustainability and competitiveness, it is important to develop catalysts based on renewable materials. Carbocatalysis is a field that has appeared in the last few years aimed at developing metal-free catalysts based on carbon.[2–4] Carbocatalysis has benefited largely from the availability of novel carbon allotropes.[3] Particularly, due to their easy preparation and remarkable properties,[5,6] graphenes are increasingly attracting interest as carbocatalysts.[2,3,7]

In the field of carbocatalysis, it is a challenge to demonstrate that materials based on carbon can act as catalysts for paradigmatic reactions promoted up to now exclusively by metals. Herein we report that graphenes, in the absence of any metal, are highly efficient carbocatalysts for the Fenton reaction. Recently, we reported that few-layers boron nitride nanoplatelets of about 20 nm lateral size can act as Fenton catalysts, although an excess of 11 equivalents of H_2O_2 was needed.[8] Boron nitride is isostructural to graphene and, therefore, it is also of interest to determine the catalytic activity of graphene materials for this reaction. A related precedent concerned the decolorization of Orange II by 200 equivalents of H_2O_2 in the presence of a reduced graphene oxide (rGO) obtained by ^{60}Co γ-ray radiation of GO in an N_2-purged sealed aqueous solution. It was claimed that the process involved the generation of HO• radicals, but no evidence for the generation of HO• radicals was provided.[9]

The Fenton reaction consists of the generation of hydroxyl radicals (HO•) by reduction of H_2O_2 promoted by Fe^{2+} [Equations (1) and (2)].[10,11] HO• is, after fluorine, the most aggressive chemical species that can exist in water, attacking virtually any organic compound. The typical application of the Fenton reaction is in the mineralization of organic pollutants in water by excess H_2O_2 at acidic pH with stoichiometric amounts of Fe^{II} salts.[11,12]

$$Fe^{2+} + H_2O_2 \rightarrow Fe^{3+} + HO + HO^- \quad (1)$$

$$Fe^{3+} + H_2O_2 \rightarrow Fe^{2+} + HOO + H^+ \quad (2)$$

Owing to concerns about water quality, the Fenton reaction has gained importance as one of the key processes for waste water remediation. The target in this reaction has been the development of catalysts that avoid the need for stoichiometric amounts of Fe^{II} salts and make efficient use of H_2O_2.[13–15] In general, catalytic Fenton processes use very large excesses of H_2O_2, commonly over 1000 equivalents with respect to pollutant.[15] It is important to show that a carbocatalyst, in the absence of any metal, can efficiently promote the Fenton reaction with quasi-stoichiometric H_2O_2 amounts. Herein we present data to show that this goal has been achieved using affordable rGO as a catalyst. rGO does not deactivate, achieving turnover numbers (TON) as high as 4540 and 15023 for phenol disappearance and H_2O_2 consumption, respectively. Based on experimental data and density functional theory (DFT) calculations, hydroquinone-like groups are proposed as active sites for the process.

To cover a range of possibilities, a series of graphenes were prepared to evaluate their activity as Fenton catalysts. The list includes GO[16] and rGO,[17] as well as a graphene sample (G)[16] and a nitrogen-doped graphene [(N)G][16,18,19] obtained by pyrolysis of alginate and chitosan, respectively. Precedents have shown that graphitic carbon residue from chitosan results after exfoliation in (N)G.[19] In addition to G and (N)G, two more boron-doped graphenes, namely (B)G and (B,N)G, obtained by pyrolysis of borate esters of alginate and chitosan, respectively, were also prepared and evaluated.[16] Pyrolysis of inorganic esters of saccharides leads to the incorporation as dopant of some heteroatom into the graphene sheet. (B)G and (N)G exhibit opposite *p*- and *n*-semiconducting properties that can be relevant in the context of H_2O_2 activation.[13–16] All of the gra-

[a] *Prof. H. García*
Instituto de Tecnología Química CSIC-UPV, Univ. Politécnica de Valencia
Av. de los Naranjos s/n, 46022 Valencia (Spain)
Center of Excellence for Advanced Materials Research
King Abdulaziz University, Jeddah (Saudi Arabia)
E-mail: hgarcia@qim.upv.es

[b] *J. C. Espinosa, Dr. S. Navalón, Dr. A. Primo, Prof. M. Álvaro*
Instituto de Tecnología Química CSIC-UPV and Departamento de Química
Univ. Politécnica de Valencia, Av. de los Naranjos s/n, 46022 Valencia (Spain)

[c] *Dr. M. Moral, Prof. J. F. Sanz*
Departamento de Química Física
Universidad de Sevilla, 41012 Sevilla (Spain)

Supporting information for this article is available on the WWW under http://dx.doi.org/10.1002/chem.201501533.

phene-based materials included in the present study have been described and fully characterized earlier.[16–19] Table S1 (see the Supporting Information) summarizes the materials discussed herein, their precursors and elemental compositions. Although the graphene materials have been obtained from different precursors and the different preparation procedures could influence their catalytic behavior beyond their composition, it is expected that their main differences are the presence of dopant elements on the graphene sheet. Spectroscopic properties of graphenes, particularly Raman and X-ray photoelectron spectroscopy (XPS), crystallinity at the microscopic level and the single layer morphology of aqueous suspensions by atomic force microscopy (AFM) have been found coincident with literature data.[16–19] All the materials exhibited the 2D, G, and D bands in Raman spectroscopy with G/D peak intensity ratio ranging from 1.3 to 1.6 (see the Supporting Information, Figure S1). XPS shows the presence of the expected dopant elements, allowing determination of their percentage (see the Supporting Information, Figures S2–S7 and Table S1). In addition, deconvolution of the C1s and N2p peaks shows for these two elements the proportion of the type of atoms present in the sample. Transmission electron microscopy (TEM) reveals high crystallinity of the samples (see the Supporting Information, Figure S8). The single-layer morphology of doped graphenes under the reaction conditions was ascertained by AFM measuring the vertical height of G sheets (see the Supporting Information, Figure S9). For the sake of comparison, commercial graphite and commercial multiwalled CNTs (MWCNTs), as well as purified and shortened MWCNTs, were also included and tested as Fenton carbocatalysts (see the Supporting Information, Table S2 and Figure S10 for their main physicochemical properties).

To evaluate the activity of graphenes as Fenton carbocatalysts, phenol was selected as a probe molecule, monitoring its disappearance with time by using 5.5 equivalents of H_2O_2. Besides phenol disappearance, the temporal profile of H_2O_2 consumption was also followed for each reaction. There have been abundant reports on the use of phenol as a probe to evaluate the activity of metal-containing catalysts, the main difference being the low H_2O_2 excess (5.5 equiv) employed here.[13–15] The temporal profile of the reaction depends on the nature of the graphene catalyst (see selected examples in Figure 1 and Figure S11 in the Supporting Information). Phenol adsorption experiments show that G and activated carbon (AC) are the solids with highest adsorption capacities (ca. 30%), followed by rGO (20%), whereas adsorption on B- and/or N-doped materials and on GO is low (<10%; see the Supporting Information, Figure S12a). The obtained adsorption values correlated with the expected strength of the π–π intermolecular forces between phenol and the adsorbent, as well as with the dispersibility of the materials in water. In the case of G, AC, and rGO, the combination of both the presence of oxygen functional groups (<25%) and the aromatic character of the materials allow a good dispersibility of the materials in water and the adsorption of phenol.[20] In contrast,

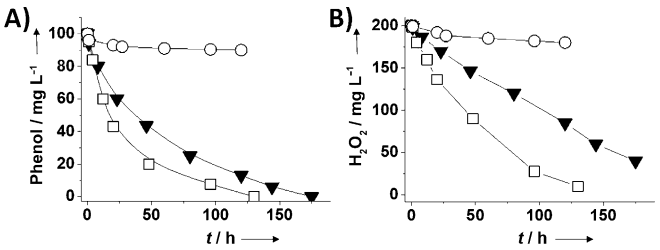

Figure 1. Temporal profiles of phenol degradation (A) and consumed H_2O_2 (B) using graphene-based catalysts. Legend: G (□), rGO (▼) and GO (○). Reaction conditions: Catalyst (200 mg L^{-1}), phenol (100 mg L^{-1}, 1.06 mM), H_2O_2 (200 mg L^{-1}, 5.88 mM), pH 3, 20 °C.

the hydrophobic character of B- or N-doped G renders more difficult their dispersibility in water and, therefore, phenol adsorption. In contrast, GO, with a high population of oxygen functional groups (ca. 50%), disperses well in water, but its high hydrophilicity makes phenol adsorption difficult. In addition, a control in the absence of any catalyst shows that neither phenol nor H_2O_2 are decomposed within the same time (see the Supporting Information, Figure S12b). Also, a control of phenol degradation was attempted in the presence of G, but in the absence of H_2O_2; no phenol conversion was observed under these conditions.

According to the results shown in Table 1, the ranking of activity of the tested carbocatalysts is G ≈ rGO > (B)G > (B,N)G > (N)G > GO. Since the catalytic activities of these graphene samples correspond to suspensions of single- or few-layer materials, this order is probably not a reflection of differences in surface area, but, most probably, on the presence of appropriate active sites. For the best catalysts, G and rGO, the temporal profiles of phenol disappearance and H_2O_2 consumption coincide, indicating that H_2O_2 is consumed exclusively in phenol degradation and not in spurious self decomposition. At the other extreme, (N)G decomposes H_2O_2 at a much higher rate than phenol ($r_0(H_2O_2)/r_0(\text{phenol}) = 160$ for (N)G) indicating that, in this case, other processes besides the Fenton reaction take place, as for the vast majority of metal catalysts reported to

Table 1. Summary of the catalytic activity for phenol degradation and H_2O_2 decomposition using graphenes as carbocatalysts.[a]

Cat.	Phenol Conv. [%]	H_2O_2 Conv. [%]	r_0(phenol) [mM h^{-1}]	$r_0(H_2O_2)$ [mM h^{-1}]	H_2O_2/phenol molar ratio[b]	E_a(phenol) [kJ mol^{-1}][c]	$E_a(H_2O_2)$ [kJ mol^{-1}][c]
G	100	95	0.042	0.147	5.2	31	31
rGO	100	80	0.038	0.146	4.3	30	30
(B)G	70	100	0.030	0.090	7.9	34	28
(N,B)G	49	100	0.023	0.170	15.1	38	24
(N)G	18	100	0.011	1.765	23.9	39	18
GO	7	3	0.002	0.009	5.5	54	48

[a] Reaction conditions: Catalyst (200 mg L^{-1}), phenol (100 mg L^{-1}, 1.06 mM), H_2O_2 (200 mg L^{-1}, 5.88 mM), pH 3, 20 °C, reaction time (Figure 1 and Figure S11 in the Supporting Information); [b] determined at final reaction time up to 150 h; [c] determined from the corresponding Arrhenius plot.

date (see Table 1).[13–15] The lack of catalytic activity of GO is remarkable and indicates that the oxygenated functional groups present on GO cannot act as active sites of the reaction. In the literature there are GO models that are compatible with the chemical analysis, ^{13}C NMR, IR and XP spectroscopic information for this material showing that the extreme oxygen content of this material ($\geq$40 wt% O) determines the presence of carboxylic acid groups, epoxides, ketones and other oxygenated functionalities with almost complete absence of aromaticity and conjugated C=C double bonds.[6,21]

In the case of (B)G, phenol disappearance exhibits an induction period, not observed for H_2O_2 consumption (see the Supporting Information, Figures S11 and S13), that is attributable to B leaching, as revealed by ICP measurements and by theoretical calculations (see the Supporting Information, Figures S13 and S14). Considering the catalytic data, rGO was the most convenient and efficient carbocatalyst for the Fenton reaction.

Analysis of the phenol decomposition products shows that hydroquinone, catechol, and *p*-benzoquinone are formed (Scheme 1). According to the accepted Fenton reaction mecha-

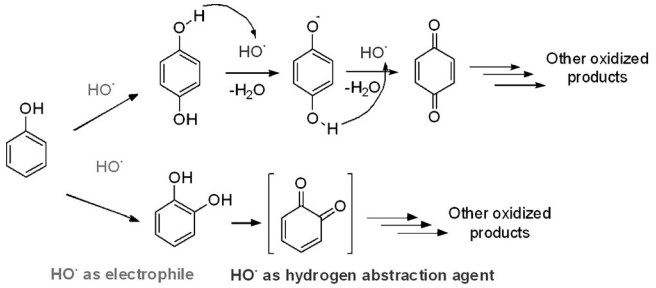

Scheme 1. Degradation pathway of phenol by hydroxyl radicals.

nism, one equivalent of phenol consumes one equivalent of HO• radicals to form catechol and hydroquinone and, then, at least two equivalents more to form *p*-benzoquinone and dicarboxylic acids. Therefore, the minimum consumption will be 3 equivalents of H_2O_2 per mole of phenol disappeared. The time-conversion plots for phenol disappearance and H_2O_2 consumption with rGO as catalyst (Figure 1) correspond to a very efficient catalyst, with $r_0(H_2O_2)/r_0(\text{phenol}) = 3.8$, indicating that at least 79% of H_2O_2 decomposes to generate HO• radicals (see the Supporting Information, Figure S15). Furthermore, by using rGO as catalyst, a H_2O_2/phenol molar ratio of 5.5 was sufficient for full degradation of phenol and its more toxic intermediates hydroquinone, *p*-benzoquinone, and catechol (see the Supporting Information, Figures S16–S18). Additional experiments were carried out with hydroquinone and catechol as starting materials. As expected, these isomeric dihydroxybenzenes were also degraded under the standard conditions employed in this work (Table 1, footnote [a], and Figure S18 in the supporting information).

One of the hallmarks of the Fenton reaction is its strong dependence on pH. In the present case, it was determined that rGO could operate within a narrow pH interval of 2–4 (see the Supporting Information, Figure S19). Lower pH values would protonate H_2O_2, disfavoring the formation of HO• radicals [Equations (3) and (4)], whereas pH values higher than 4 would increase the concentration of hydroperoxy anions, leading to a decrease of both H_2O_2 and HO• radical concentrations [Equations (5) and (6)].[22] Also, increasing the pH decreases the oxidation potential of HO• radicals.

pH < 2

$$H_2O_2 + H^+ \rightarrow H_3O_2^+ \quad (3)$$

$$HO^\bullet + H^+ + e^- \rightarrow H_2O \quad (4)$$

pH > 4

$$H_2O_2 + HOO^- \rightarrow H_2O + O_2 + HO^\bullet \quad (5)$$

$$HO^\bullet + HOO^- \rightarrow H_2O + O_2^{\bullet -} \quad (6)$$

The stability and maximum productivity of a catalyst are crucially important. To prove the stability and determine the productivity of rGO, a series of consecutive reuses were performed in which the ratio of phenol (1000 mg L^{-1}) to rGO (50 mg L^{-1}) was increased by a factor of 40, allowing the reaction to run for long times (see the Supporting Information, Figure S20). Five consecutive reuses were measured, whereby phenol and H_2O_2 concentrations as high as 3.95 and 4.73 g L^{-1}, respectively, reacted with only 50 mg L^{-1} of rGO (one quarter the rGO amount employed in the general reaction procedure). The slight increase in catalytic activity observed upon reusing rGO was attributed to the better rGO dispersibility in water upon reuse due to mild rGO hydroxylation (see the Supporting Information, Figure S21). It should be noted that the residual oxygen content of rGO (ca. 15 wt%) makes possible its dispersion in aqueous phase by sonication to test its catalytic activity. Normally, although GO is highly dispersible in water due to its hydrophilicity, reduction of GO to rGO decreases considerably the hydrophilicity. In the present case, owing to the residual O content of rGO, it remains dispersible in water.[20] However, after its use as Fenton catalyst, it was noticed that just stirring or light sonication was sufficient to obtain a permanent suspension of used rGO. Importantly, a H_2O_2/phenol molar ratio of only 3.3 was needed for complete phenol degradation. Again, in the absence of catalyst the reaction did not take place (see the Supporting Information, Figure S20). Unfortunately, the unknown nature of the active centers in rGO precludes the precise determination of turnover number (TON). Nevertheless, it has been established by XPS that quinone centers in rGO can account for about 2–5 wt%.[23] As discussed below, quinone centers are possible active sites and their percentage can be estimated based on the deconvolution of the experimental C1s peak to individual components and quantification of the percentage of C=O carbons. Speculating that the percentage of active centers is in this proportion, based on XPS quantification of the fraction of C=O, then, an estimation of the accumulated TON achieved with rGO as a carbocatalyst would be 4540 and 15023 for phenol disappearance and H_2O_2 consumption,

respectively. This TON is higher than those reported for many transition metal Fenton catalysts,[13,15] although it is still about two orders of magnitude lower than that reported for the best Fenton catalyst, based on supported Au NPs (458459).[24,25] Carbocatalysts based on G are, however, still open to further optimization by material engineering and the accumulated TON value measured is just the first estimation in this area. Graphene samples specially engineered for optimized quinone-like content, instead of just a few percent, should exhibit an optimal catalytic activity.

It should be noted that, besides hydroquinone/quinone-like redox pairs, there could also be other possible sites on doped G to promote the reaction. In the case of (N)G we have seen that there is a considerable decomposition of H_2O_2 that is not associated to the generation of HO$^{\bullet}$ radicals, in accordance with previous reports in the literature.[26] These sites are probably some of the different types of N atoms present in (N)G. In the case of (B)G, it was found that B atoms are not stable on G and decompose spuriously H_2O_2 while the B atoms are leached. This indicates again that B atoms are sites for H_2O_2 decomposition.

Importantly, the possibility that traces of Mn were responsible for the observed activity during the productivity tests was dismissed by performing additional productivity experiments in which Mn^{2+} ions were deliberately added in a range of ppm concentrations (50 μg), both in the presence and in the absence of rGO, leading to a lack of activity (in the absence of rGO) or no variation with respect to the use of rGO (Mn impurity content <100 ppm; see the Supporting Information, Figure S22). It should also be noted that GO (not rGO) is the sample with the highest Mn^{2+} contamination (150 ppm) and is, however, the less active (Table 1). Thus, there is no apparent relationship between the possible metal impurities and the activity.

The activation energy (E_a) of phenol disappearance and H_2O_2 decomposition was estimated for a series of graphenes by performing the reaction at different temperatures from 20 to 80 °C (Table 1, Figure 2, and Figures S23–S27 in the Supporting Information). It was observed that the E_a for the most efficient catalyst for phenol disappearance and H_2O_2 decomposition has a coincident value of 30 kJ mol^{-1}.

The fact that the two processes exhibit the same E_a is in agreement with the exclusive operation of a Fenton reaction

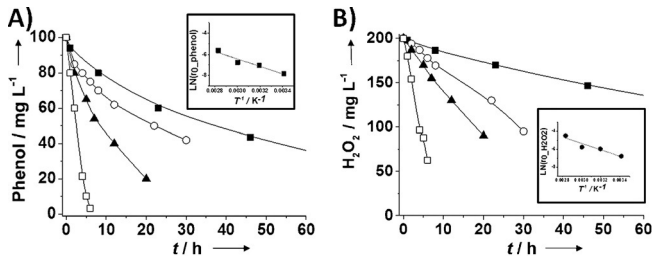

Figure 2. (A) Phenol degradation and (B) H_2O_2 decomposition as a function of the reaction temperature using rGO as catalyst. The insets show the Arrhenius plots for both processes. Reaction conditions: Catalyst (200 mg L^{-1}), phenol (100 mg L^{-1}, 1.06 mM), H_2O_2 (200 mg L^{-1}, 5.88 mM), pH 3. Legend: 80 °C (□), 60 °C (▲), 40 °C (○) and 20 °C (■).

in which generation of HO$^{\bullet}$ radical from H_2O_2 will be the rate determining step, responsible for the E_a. Once HO$^{\bullet}$ radicals are generated, they react with phenol or dihydroxybenzenes essentially without an energy barrier and, consequently, the E_a of phenol degradation and generation of HO$^{\bullet}$ radicals would coincide. Also remarkable is that the E_a value is relatively low and comparable with that reported for the most efficient heterogeneous Fenton catalyst based on Au NPs supported on diamond nanoparticles.[25] For less efficient carbocatalysts such as (N)G, the E_a values of phenol degradation are higher than those of H_2O_2 decomposition, implying that the barrier to decompose H_2O_2 is lower and the attack of phenol requires additional activation. This mismatch between lower E_a for H_2O_2 decomposition and higher E_a for phenol disappearance increases as the efficiency of the catalyst to generate HO$^{\bullet}$ radicals decreases.

The efficiency of rGO to generate HO$^{\bullet}$ radicals in the decomposition of H_2O_2 can be estimated by performing an experiment in which phenol is in large excess with respect to H_2O_2. Conditions using a large excess of phenol are the opposite to those generally used when the target is to degrade phenol, but under these reverse conditions most of the HO$^{\bullet}$ radicals would attack preferentially phenol forming catechol, hydroquinone, and *p*-benzoquinone and, by quantifying these products with respect to H_2O_2 consumption, the percentage of decomposed H_2O_2 that has generated HO$^{\bullet}$ radicals can be indirectly determined (Scheme 1). Measurements under these conditions have established that at least 82% of H_2O_2 consumption is correlated with the transformation of phenol to catechol, hydroquinone and *p*-benzoquinone (see the Supporting Information, Figures S18a and S28). As the reaction proceeds, this efficiency apparently decreases due to the reaction of HO$^{\bullet}$ radicals with the primary products rather than with phenol. This efficiency in the generation of HO$^{\bullet}$ radical is remarkably high and justifies why there is no need of a large H_2O_2 excess for phenol degradation.

Evidence of the generation of HO$^{\bullet}$ radicals was indirectly obtained by dimethylsulfoxide (DMSO) quenching of phenol degradation. DMSO is known to react readily with HO$^{\bullet}$ radicals, leading to the formation of $CH_3^{\bullet}$ radicals and methanesulfinic acid [Equation (7)].[27] DMSO quenching experiments under appropriate conditions with rGO as catalyst show that phenol degradation is completely inhibited by a tenfold molar excess of DMSO, thus proving indirectly the mechanism of the Fenton reaction (see the Supporting Information, Figure S29).

$$(CH_3)_2SO + OH \rightarrow CH_3SO_2H + CH_3 \quad (7)$$

Further evidence for the generation of HO$^{\bullet}$ radicals was obtained by electron paramagnetic resonance (EPR) spectroscopy with phenyl-α-*tert*-butyl nitrone (PBN) as a trapping agent. The EPR spectra of the corresponding PBN–(OH) adduct radical were recorded (Figure 3). This EPR spectrum, with fine structure giving structural information, constitutes firm evidence of HO$^{\bullet}$ radical generation from H_2O_2 by rGO. It should, however, be noted that EPR spectroscopy with PBN as HO$^{\bullet}$ radical trap is not a suitable procedure to quantify the percentage of HO$^{\bullet}$

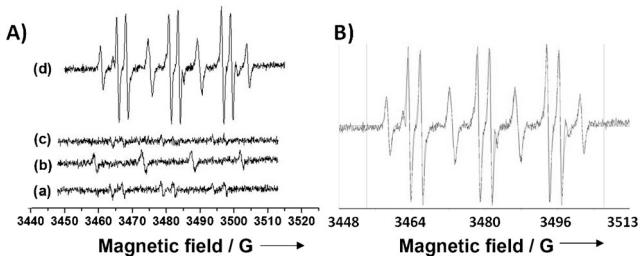

Figure 3. (A) EPR spectra of (a) PBN + H_2O; (b) rGO + PBN; (c) PBN + H_2O_2; (d) rGO + H_2O_2 + PBN. (B) EPR spectra of sample (d) and its fitting considering the PBN-OH adduct (AG_N = 15.5 and AG_H = 2.7) and *tert*-butyl aminoxyl (AG_N = 14.58 and AG_H = 13.90) coinciding with the reported values in the literature. EPR reaction conditions: rGO (200 mg L^{-1}), PBN (1,041 mg L^{-1}, 5.88 mM), PBN/H_2O_2 molar ratio = 1:1, pH 3, 45 min reaction time.

radical generated by each G catalyst due to degradation of PBN by HO• radicals. Thus, PBN trapping of HO• can only be taken as a procedure for HO• detection.

To provide some conceptual framework to rationalize the catalytic activity of graphenes for the Fenton reaction, basic DFT calculations were performed with simple models of hydroquinone moieties that could be present in G. It is pertinent to comment that prior DFT calculations predicted that graphenic N atoms on G [for (N)G] decompose H_2O_2 to H_2O via N-OH intermediates.[26] In line with these calculations that were not supported experimentally, herein it has been observed that (N)G effects a considerable degree of H_2O_2 decomposition without generating free HO• radicals in solution.

Our DFT study started by calculating the feasibility of HO• generation by hydroquinone-mediated H_2O_2 reduction (Scheme 2). The calculations indicate that the process is uphill by approximately 2 eV in a difference of terms of about 130 eV. Similar calculations predict that the presence of electron donor

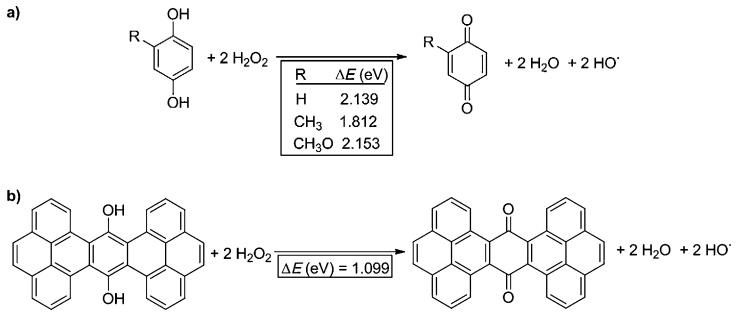

Scheme 2. Energy variation (DE) in the generation of HO• radicals from H_2O_2 by hydroquinones as models of graphene active sites.

substituents in the aromatic ring decreases the endoergonicity of the process to about 0.16 eV. Another model of hydroquinone-like moieties present on G having condensed benzopyrene units shows again that HO• generation from H_2O_2 reduction of hydroquinone moieties should be slightly unfavorable by 1.1 eV in a difference of terms about 400 eV. Overall, these DFT calculations indicate that the process of HO• generation from hydroquinones is quasi-neutral from the energy viewpoint, this situation being ideal for site reversibility. It is clear that further calculations are necessary using more extended model structures of G and addressing the various steps in the reaction mechanism for a better understanding of the origin of the Fenton-like catalytic activity on graphenes.

To provide some support to this prediction about the nature of the redox sites on G, we selected *p*-benzoquinone and hydroquinone as simple model molecules present in the rGO structure. With these two molecules as organocatalysts, the catalytic activity for both phenol degradation and H_2O_2 decomposition was evaluated (see the Supporting Information, Figures S30–S32). The two organocatalysts behaved similarly, promoting the Fenton reaction. In addition, DMSO quenching and PBN trapping (see the Supporting Information, Figures S32 and S33) of HO• radicals also confirmed that HO• radicals are generated by reduction of H_2O_2 with hydroquinone. Similarly, 2-methoxyhydroquinone and 2-methylhydroquinone as organocatalysts also generate HO• radicals by reduction of H_2O_2, as demonstrated by DMSO quenching experiments (see the Supporting Information, Figure S34), at a greater rate than the parent hydroquinone, in good agreement with the predicted influence of electron donor substituents (Figure S34).

Finally, we evaluated the catalytic activity of rGO versus that of other carbonaceous materials, such as graphite, MWCNT, and derivatives. Other carbon materials were also found to exhibit catalytic activity for the Fenton degradation of phenol (see the Supporting Information, Figure S35). Particularly notable is the catalytic activity of purified, short CNTs that for phenol degradation is similar to that of rGO. It should be noted, however, that, during the process, CNTs consume a significantly larger amount of H_2O_2 and, therefore, the catalytic activity of rGO is much better than those of graphite and MWCNTs in terms of high efficiency in HO• generation. As mentioned earlier, the optimal Fenton catalyst should exhibit complete selectivity of H_2O_2 decomposition into OH• radicals, and this requires that the E_a for phenol consumption and H_2O_2 decomposition should be equal and that the number of equivalents of H_2O_2 consumed be minimal and close to the theoretical value. With regard to the catalytic activity of graphite, it has been possible to detect the presence of G at final reaction times. Thus, graphite might act as a precursor of some active G. This hypothesis is consistent with the observation in the time-conversion plot of an initial induction period (see Figure S34 in the supporting information). Another point to note is the benefit of oxidative treatment of MWCNT, a fact that can be attributed to the generation of oxygenated functional groups such as quinone- and/or hydroquinone-like groups (see the Supporting Information, Table S2 and Figure S10).[28] It should be noted, however, that not all of the oxygenated functional groups should be active centers for Fenton-like H_2O_2 decomposition and that, according to our proposal, only those hydroquinone/quinone subunits of adequate redox potential would act as sites for HO• radical generation, whereas other oxygenated functional groups can decom-

pose H_2O_2 into O_2 without forming HO• radicals. In contrast, AC exhibited negligible activity as a carbocatalyst for phenol degradation, while promoting the decomposition of H_2O_2. The apparent phenol removal observed for AC corresponds merely to adsorption (see the Supporting Information, Figure S35). In any case, the data obtained on the general activity of carbon materials (particularly those with graphene structures) combined with the previously discussed activity of *p*-benzoquinone and substituted hydroquinones show that the concept of carbocatalysis to promote the Fenton reaction is of universal application and could lead to the development of a vast number of metal-free catalysts. For comparison, under the present conditions, a noble metal benchmark catalyst based on Au NPs (1 wt%; 10.8 nm average) supported on Fenton-treated diamond nanoparticles promotes the complete phenol degradation by H_2O_2 as oxidant at pH 4 in about 50 h.[24] Although less active, G or rGO, as metal free-catalysts, effected this transformation in about 150 h at pH 3 (Figure 1) and could represent an example of replacing noble metals by other cost-effective carbocatalysts.

In conclusion, herein we have shown that graphenes can act as carbocatalysts for the Fenton generation of HO• from H_2O_2, a reaction that, to date, has been reported exclusively using transition metal catalysts. The composition and structure of the G sample influence its catalytic activity that is maximal for rGO and G. In these cases, a minimum selectivity towards HO• formation of 82% was estimated and very large productivity values with even an increase in activity upon reuse and optimal H_2O_2 consumption were established. The concept of metal-free catalysts for Fenton reaction was shown to be universal and such catalysts can be based on those materials that contain certain oxygenated functional groups that act as redox centers with the correct potential to oxidize and reduce H_2O_2.

Acknowledgements

Financial support by Generalidad Valenciana (GV/2013/040 and Prometeo 2012/2013) is gratefully acknowledged. Spanish Ministry of Economy and Competitiveness is also thanked for funding (Severo Ochoa and CTQ2012-32315).

Keywords: carbon · fenton reaction · graphene · heterogeneous catalysis · radicals

[1] M. Stratakis, H. Garcia, *Chem. Rev.* **2012**, *112*, 4469 – 4506; R. Jana, T. P. Pathak, M. S. Sigman, *Chem. Rev.* **2011**, *111*, 1417 – 1492; T. Punniyamurthy, S. Velusamy, J. Iqbal, *Chem. Rev.* **2005**, *105*, 2329 – 2363; S. Navalón, M. Alvaro, H. Garcia, *ChemCatChem* **2013**, *5*, 3460 – 3480.

[2] D. R. Dreyer, C. W. Bielawski, *Chem. Sci.* **2011**, *2*, 1233 – 1240; C. Su, K. P. Loh, *Acc. Chem. Res.* **2013**, *46*, 2275 – 2285; D. S. Su, S. Perathoner, G. Centi, *Chem. Rev.* **2013**, *113*, 5782 – 5816.

[3] S. Navalon, A. Dhakshinamoorthy, M. Alvaro, H. Garcia, *Chem. Rev.* **2014**, *114*, 6179 – 6212.

[4] X.-K. Kong, C.-L. Chen, Q.-W. Chen, *Chem. Soc. Rev.* **2014**, *43*, 2841 – 2857.

[5] D. R. Dreyer, R. S. Ruoff, C. W. Bielawski, *Angew. Chem. Int. Ed.* **2010**, *49*, 9336 – 9344; *Angew. Chem.* **2010**, *122*, 9524 – 9532.

[6] D. R. Dreyer, S. Park, C. W. Bielawski, R. S. Ruoff, *Chem. Soc. Rev.* **2010**, *39*, 228 – 240.

[7] A. Schaetz, M. Zeltner, W. J. Stark, *ACS Catal.* **2012**, *2*, 1267 – 1284; D. R. Dreyer, H.-P. Jia, C. W. Bielawski, *Angew. Chem. Int. Ed.* **2010**, *49*, 6813 ; *Angew. Chem.* **2010**, *122*, 6965 – 6816.

[8] A. Primo, S. Navalón, A. M. Asiri, H. García, *Chem. Eur. J.* **2015**, *21*, 324 – 330.

[9] Y. Zhao, W.-F. Chen, C.-F. Yuan, Z.-Y. Zhu, L.-F. Yan, *Chin. J. Chem. Phys.* **2012**, *25*, 335 – 338.

[10] J. J. Pignatello, E. Oliveros, A. Mackay, *Crit. Rev. Environ. Sci. Technol.* **2006**, *36*, 1 – 84.

[11] E. Neyens, J. Baeyens, *J. Hazard. Mater.* **2003**, *98*, 33 – 50.

[12] M. Pera-Titus, V. García-Molina, M. A. Baños, J. Giménez, S. Esplugas, *Appl. Catal. B* **2004**, *47*, 219 – 256.

[13] S. Navalon, M. Alvaro, H. Garcia, *Appl. Catal. B* **2010**, *99*, 1 – 26.

[14] S. Navalon, A. Dhakshinamoorthy, M. Alvaro, H. Garcia, *ChemSusChem* **2011**, *4*, 1712 – 1730.

[15] A. Dhakshinamoorthy, S. Navalon, M. Alvaro, H. Garcia, *ChemSusChem* **2012**, *5*, 46 – 64.

[16] A. Dhakshinamoorthy, A. Primo, P. Concepción, M. Alvaro, H. García, *Chem. Eur. J.* **2013**, *19*, 7547 – 7554.

[17] L.-Y. Meng, S.-J. Park, *Adv. Mater. Res.* **2010**, *123 – 125*, 787 – 790; C. D. Zangmeister, *Chem. Mater.* **2010**, *22*, 5625 – 5629; M. Jin, H.-Y. Jeong, T.-H. Kim, K. P. So, Y. Cui, W. J. Yu, E. J. Ra, Y. H. Lee, *J. Phys. D* **2010**, *43*, 275402.

[18] A. Primo, P. Atienzar, E. Sanchez, J. M. Delgado, H. García, *Chem. Commun.* **2012**, *48*, 9254 – 9256.

[19] A. Primo, E. Sanchez, J. M. Delgado, H. García, *Carbon* **2014**, *68*, 777 – 783.

[20] D. Koniosa, M. M. Stylianakis, E. Stratakis, E. Kymakis, *J. Colloid Interface Sci.* **2014**, *430*, 108 – 112.

[21] D. R. Dreyer, A. D. Todd, C. W. Bielawski, *Chem. Soc. Rev.* **2014**, *43*, 5288 – 5301.

[22] A. Mahmood, S. Ali, H. Saleem, T. Hussain, *Asian J. Chem.* **2011**, *23*, 3875 – 3878; C. M. Silva, P. L. Silva, J. R. Pliego, *Int. J. Quantum Chem.* **2014**, *114*, 501 – 507; J.-H. Sun, S.-P. Sun, G.-L. Wang, L.-P. Qiao, *Dyes Pigm.* **2007**, *74*, 647 – 652.

[23] A. Bagri, C. Mattevi, M. Acik, Y. J. Chabal, M. Chhowalla, V. B. Shenoy, *Nat. Chem.* **2010**, *2*, 581 – 587; S. Choudhary, H. P. Mungse, O. P. Khatri, *Chem. Asian J.* **2013**, *8*, 2070 – 2078.

[24] S. Navalon, R. Martin, M. Alvaro, H. Garcia, *Angew. Chem. Int. Ed.* **2010**, *49*, 8403 – 8407; *Angew. Chem.* **2010**, *122*, 8581 – 8585.

[25] R. Martin, S. Navalon, J. J. Delgado, J. J. Calvino, M. Alvaro, H. Garcia, *Chem. Eur. J.* **2011**, *17*, 9494 – 9502.

[26] P. Wu, P. Du, H. Zhang, C. Cai, *Phys. Chem. Chem. Phys.* **2013**, *15*, 6920 – 6928.

[27] M. J. Burkitt, R. P. Mason, *Proc. Natl. Acad. Sci. USA* **1991**, *88*, 8440 – 8444; S. Navalon, R. Martin, M. Alvaro, H. Garcia, *ChemSusChem.* **2011**, *4*, 650 – 657; S. Navalon, D. Sempere, M. Alvaro, H. Garcia, *ACS Appl. Mater. Interfaces* **2013**, *5*, 7160 – 7169.

[28] P. Slobodian, P. Riha, P. Cavallo, C. A. Barbero, R. Benlikaya, U. Cvelbar, D. Petras, P. Saha, *J. Nanomater.* **2014**, *2014*, Article ID 589627; J. Zhang, H. Zou, Q. Qing, Y. Yang, Q. Li, Z. Liu, X. Guo, Z. Du, *J. Phys. Chem. B* **2003**, *107*, 3712 – 3718; D. B. Mawhinney, V. Naumenko, A. Kuznetsova, J. J. T. Yates, *J. Am. Chem. Soc.* **2000**, *122*, 2383 – 2374.

Received: April 20, 2015
Published online on July 16, 2015